CHEMISTRY OF MATERIALS
Article

Chem. Mater. **2011,** *23,* 913–922 913
DOI:10.1021/cm102736d

Organic Porphyrin Nanoparticles with Induced Optical Activity: Ion-Based Synthesis from Achiral Chromophore and Chiral Counterions†

Hiroshi Yao,* Hisamu Sasahara, and Keisaku Kimura

Graduate School of Material Science, University of Hyogo, 3-2-1 Koto, Kamigori-cho, Ako-gun, Hyogo 678-1297, Japan

Received September 23, 2010. Revised Manuscript Received November 16, 2010

Organic porphyrin nanoparticles with induced optical activity are successfully synthesized via ion-association between the achiral *meso*-tetrakis(1-methylpyridinium-4-yl) porphine (TMPyP) cation and the chiral hexacoordinated phosphate (D_3-symmetric TRISPHAT or C_2-symmetric BINPHAT with Δ or Λ chirality, respectively) anion in the presence of poly(vinylpyrrolidone). The particle size ranges from 30 to 50 nm in diameter, which is almost independent of the counteranion used. The Soret band of the porphyrin nanoparticles exhibits a large bathochromic shift in comparison with that of the porphyrin monomer in solution. Simple quantum chemical calculations suggest that the *meso*-substituent flattening of the TMPyP molecule as well as ruffling/saddling deformation can be an origin of this bathochromic shift. The induced circular dichroism (CD) of the porphyrin nanoparticles exhibits split Cotton effects at the Soret band region, although the split modes are different between the nanoparticles prepared from TMPyP/TRISPHAT and TMPyP/BINPHAT systems. Possible mechanisms that could account for the chiroptical effects observed in the porphyrin nanoparticles are also discussed. We believe this synthetic concept and methodology are applicable to a wide variety of dyes and thus will be attractive to produce optically active organic nanoparticles with simplicity and versatility.

Introduction

The successful development of molecular devices for applications in photochemical energy conversion/storage and optoelectronic systems requires fundamental research of photofunctional organic materials.[1] Recent research entails photophysical/photochemical investigations of noncovalent organic assemblies or aggregates on nanometer scales because their photofunctionality significantly differs from that of the isolated monomers.[2] In particular, porphyrins are attractive organic building blocks for photofunctional nanoarchitectures, because they are remarkably robust under a variety of conditions and have interesting photophysical, photochemical, and redox properties that can be readily fine-tuned by substituents or by metal ions in the center of the macrocycle.[3] With the appropriate selection of porphyrin structures, the noncovalent self-assembly can be fabricated via intermolecular electrostatic interaction, hydrogen bonding, and/or metal coordination.[3]

Porphyrin nanoparticles, as one of the noncovalent assemblies, have also received increasing interest for both pharmaceutical and materials applications, and been prepared by adding a guest solvent, in which the porphyrin is insoluble, to a solution of the macrocycle in a host solvent with a small percentage of polyethylene glycol as a stabilizer and vigorous mixing (reprecipitation method).[4,5] The particle size (10−100 nm in diameter) and chromophore organization depended on the molecular structure and the conditions used to form the nanoparticles. We have also succeeded in synthesizing porphyrin nanoparticles with narrow size distribution using an ion-association method, and the absence of chromophore self-aggregation was a characteristic feature of our system, representing unique spectroscopic properties.[6]

Meanwhile, the control and tuning of chirality at the supramolecular (or nanoscopic) level is a field of ever growing interest.[7] In particular, studies on controlling chirality in porphyrin-based nanoarchitectures constitute

†Accepted as part of the "Special Issue on π-Functional Materials".
*Corresponding author. Fax: +81-791-58-0161. E-mail: yao@sci.u-hyogo.ac.jp.

(1) (a) Aviram, A.; Ratner, M. A. *Chem. Phys. Lett.* **1974**, *29*, 277. (b) Keyes, R. W. *Phys. Today* **1992**, *45*, 42.
(2) (a) Belanger, S. S.; Hupp, J. T. *Angew. Chem., Int. Ed.* **1999**, *38*, 2222. (b) Stang, P. J.; Olenyuk, B. *Acc. Chem. Res.* **1997**, *30*, 502. (c) Rotomskis, R.; Augulis, R.; Snitka, V.; Valiokas, R.; Liedberg, B. *J. Phys. Chem. B* **2004**, *108*, 2833. (d) Marks, T. J. *Science* **1985**, *227*, 881.
(3) (a) Dolphin, D. *The Porphyrins*; Academic Press: New York, 1978, Vols. *I*−*VII*. (b) Drain, C. M.; Varotto, A.; Radivojevic, I. *Chem. Rev.* **2009**, *109*, 1630.
(4) Gong, X.; Milic, T.; Xu, C.; Batteas, J. D.; Drain, C. M. *J. Am. Chem. Soc.* **2002**, *124*, 14290.
(5) (a) Drain, C. M.; Smeureanu, G.; Patel, S.; Gong, X.; Garno, J.; Arijeloye, J. *New J. Chem.* **2006**, *30*, 1834. (b) Kasai, H.; Nalwa, H. S.; Oikawa, H.; Okada, S.; Matsuda, H.; Minami, N.; Kakuta, A.; Ono, K.; Mukoh, A.; Nakanishi, H. *Jpn. J. Appl. Phys. Part-2* **1992**, *31*, L1132.
(6) (a) Ou, Z.; Yao, H.; Kimura, K. *J. Photochem. Photobiol. A* **2007**, *189*, 7. (b) Ou, Z.; Yao, H.; Kimura, K. *Chem. Lett.* **2006**, *35*, 782.
(7) (a) Amabilino, D. B. *Chem. Soc. Rev.* **2009**, *38*, 669. (b) Crassous, J. *Chem. Soc. Rev.* **2009**, *38*, 830. (c) Matheos-Timoneda, M. A.; Crego-Calama, M.; Reinhoudt, D. N. *Chem. Soc. Rev.* **2004**, *33*, 363.

Published on Web 02/01/2011

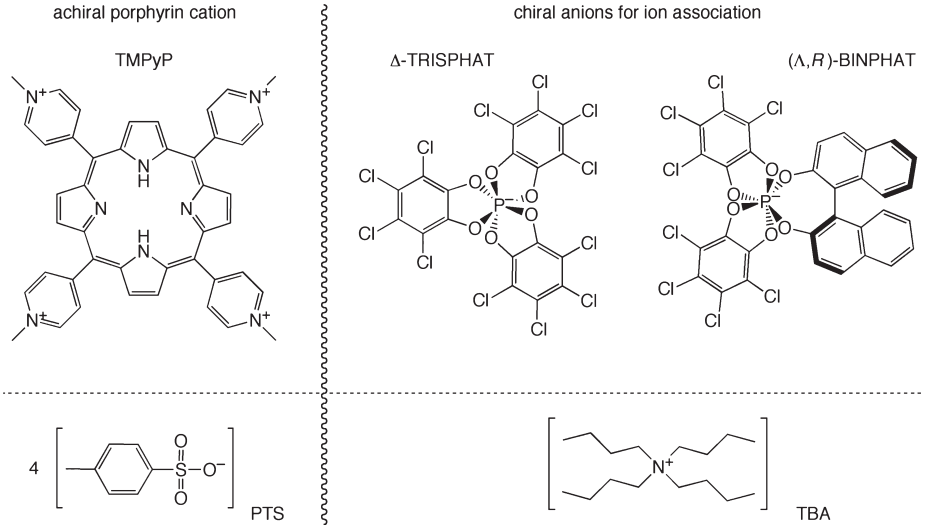

Figure 1. Chemical structures of TMPyP, TRISPHAT, and BINPHAT. The native counterions are also presented.

a mandatory step for the construction of systems mimicking biological functions[8] such as cytochrome P-450 activity, or myoglobin and hemoglobin functions (for example, myoglobin, an oxygen-binding compact heme protein, exhibits characteristic circular dichroism (CD) induced by the surrounding chiral protein, providing significant information on the local asymmetric structure around heme).[9] Generally, the methods to make artificial porphyrin chiral nanoarchitectures include; (i) use of intrinsically chiral chromophores, or (ii) use of achiral chromophores in the presence of chiral templates or environments.[10] In both strategies, it is important to understand the principles and conditions that may lead to the construction of chiral nanoarchitectures of high structural integrity and tunable functionality.

Again, we have developed a new route for the synthesis organic nanoparticles in solution based on the ion-association technique that has advantages in simplicity and versatility.[11] This method utilizes the formation of water-insoluble ion-pair aggregates in aqueous solution by association of a chromophoric ion with a hydrophobic counterion to fabricate organic nanoarchitectures. Using this approach, we are able to design and produce artificial porphyrin chiral nanostructures or nanoparticles by optimizing the interionic interaction between an achiral porphyrin chromophore and the large counterion with chirality. Herein we report the synthesis and optical/chiroptical properties of asymmetrically transformed porphyrin nanoparticles. *Meso*-tetrakis(1-methylpyridinium-4-yl) porphine (TMPyP) is selected as the achiral cationic dye with a circular dichroism (CD) reporter. A bulky hexacoordinated phosphate anion with Λ or Δ chirality in left- or right-handed propeller shape (*M* or *P* helicity), respectively,[12] is then associated with the TMPyP cation in the presence of a neutral polymer stabilizer poly(vinylpyrrolidone) in solution, yielding organic porphyrin nanoparticles of about 30−50 nm with induced optical activity. Structural implications of the porphyrin chromophore that are related to optical and chiroptical properties of the nanoparticles are discussed.

Experimental Section

Materials. Achiral *meso*-tetrakis(1-methylpyridinium-4-yl) porphine (abbreviated as TMPyP; chemical structure is shown in Figure 1) tetra-*p*-toluenesulfonate (PTS), tetrabutylammonium (TBA) salts of D_3-symmetric Δ-tris(tetrachloro-1,2-benzenediolato)-phosphate(V) and C_2-symmetric (Λ,*R*)-(1,1′-binaphthalene-2,2′-diolato)(bis(tetrachlor-1,2-benzenediolato))phosphate(V) (TRISPHAT and BINPHAT, respectively; see also Figure 1), as well as TBA•PTS (tetrabutylammonium *p*-toluenesulfonate), were purchased from Sigma-Aldrich Chemical Co. and used as received. Poly(vinylpyrrolidone) (PVP; average M_W = 10 000, Aldrich) was used as a neutral stabilizer to prevent particle agglomeration. Methanol (GR grade) and ethanol (GR grade) were received from Wako Pure Chemical and used as received. Pure water was obtained by an Advantec GS-200 automatic water-distillation supplier.

Instrumentation. Morphology and size of the nanoparticles were examined with a Hitachi S-4800 scanning transmission electron microscope (STEM). A specimen for STEM observations was prepared by dropping the suspension on an amorphous carbon-coated copper mesh. The hydrodynamic diameter measurements of nanoparticles on the basis of dynamic light scattering (DLS) were conducted with an Otsuka ELS-800 light scattering spectrophotometer with a 10-mW He−Ne laser. Crystallinity of the solid-state products was examined with a polarized-light microscope (BXP; Olympus) with cross polarizers because it gives us significant information on the structural anisotropy with birefringence.[13] UV−visible absorption spectra

(8) (a) Pasternack, R. F.; Fleming, C.; Herring, S.; Collings, P. J.; dePaula, J.; DeCastro, G.; Gibbs, E. J. *Biophys. J.* **2000**, *79*, 550. (b) Pasternack, R. F.; Gibbs, E. J.; Bruzewicz, D.; Stewart, D.; Engstrom, K. S. *J. Am. Chem. Soc.* **2002**, *124*, 3533.
(9) (a) Ortiz de Montellano, P. R. *Cytochrome P-450: Structure, Mechanism and Biochemistry*, 2nd ed.; Plenum: New York, 1995. (b) Philipson, K. D.; Tsai, S. C.; Sauer, K. *J. Phys. Chem.* **1971**, *75*, 1440. (c) Houssier, C.; Sauer, K. *J. Am. Chem. Soc.* **1970**, *92*, 779.
(10) Lauceri, R.; Raudino, A.; Scolaro, L. M.; Micali, N.; Purrello, R. *J. Am. Chem. Soc.* **2002**, *124*, 894.
(11) (a) Yao, H.; Ou, Z.; Kimura, K. *Chem. Lett.* **2005**, *34*, 1108. (b) Ou, Z.; Yao, H.; Kimura, K. *Bull. Chem. Soc. Jpn.* **2007**, *80*, 295. (c) Yao, H.; Yamashita, M.; Kimura, K. *Langmuir* **2009**, *25*, 1131.
(12) Lacour, J.; Frantz, R. *Org. Biomol. Chem.* **2005**, *3*, 15.
(13) Yao, H.; Domoto, K.; Isohashi, T.; Kimura, K. *Langmuir* **2005**, *21*, 1067.

were recorded on a Hitachi U-4100 spectrophotometer. Circular dichroism (CD) spectra were recorded with a JASCO J-820 spectropolarimeter. Rectangular 1 cm cuvettes made of quartz were used for the measurements.

Methods. *1. From Achiral Porphyrin to Anion-Induced Optically Active Organic Nanoparticles: Ion-Association Synthesis.* Organic porphyrin nanoparticles with induced optical activity were prepared by means of the "ion-association" technique.[11] A typical preparation procedure is depicted as follows: At room temperature, rapid addition of aqueous PVP solution (1.8 mL; [PVP] = 0.2 mg/mL) into the ultrasonicated methanol solution of 0.2 mL containing both native TMPyP (PTS salt) and native TRISPHAT (or BINPHAT) (TBA salt), at the molar ratio of 1:4 or 1:6, produced almost clear pale yellow suspension of porphyrin-based nanoparticles.[14] The net charge ratio (determined as ρ) of the loaded phosphate anion to the present TMPyP, that is, [phosphate]/(4 × [TMPyP]), was then 1 or 1.5. Note that the native hexacoordinated phosphate compounds, TBA salts of TRISPHAT and BINPHAT, did not dissolve in pure water but TBA·PTS was soluble in water, so that the nanoparticle products composed of ion-pair adducts (TMPyP/TRISPHAT and TMPyP/BINPHAT) were consequently dispersed in the water/methanol (9/1 v/v) mixture. Ultrasonication was further continued for 10 min. The sample was then allowed to stand overnight. We call these products "TMPyP nanoparticles" because their spectroscopic properties are dominated by the porphyrin chromophore. To be concise, we refer to the TMPyP nanoparticle sample prepared using TRISPHAT or BINPHAT as TMPyP-**T** or TMPyP-**B**, respectively.

2. Ion-Pair Precipitates. In the absence of PVP, the preparation procedures at the charge ratio of ρ = 1 gave yellow precipitates of ion-pair adducts between TMPyP and the chiral phosphate.[14] We first observed the solid precipitates using a polarized-light microscope to check whether they are crystalline or amorphous. Next, the solution containing the precipitates was filtered by a 200 nm pore size membrane filter (Millipore, Millex-FG; SLFG025LS). The filtrated (supernatant) solution, which was completely colorless and transparent, was examined by UV−vis spectroscopy. The yellow solids collected onto the filter membrane were dried in vacuum, followed by washing with water completely. Injection of methanol or ethanol into the membrane filter yielded transparent yellow solution, which was also examined by UV−vis spectroscopy.

3. Computational Methods. Ground-state geometry calculations of TMPyP, TRISPHAT, BINPHAT, TMPyP−TRISPHAT (1:1 complex) and TMPyP−BINPHAT (1:1 complex) were carried out with the Gaussian 03 program[15] at the semiempirical PM3 level. For calculations of the 1:1 complex, we chose initial guess geometries of $TMPyP^{4+}$ with one of the counteranions ($TRISPHAT^-$ or $BINPHAT^-$) located at the vicinity of the positively charged methylpyridinium position. The electrostatic potential surface, an overlaying of the electrostatic potential (the attraction or repulsion of a positive charge) onto the electron density, was also obtained for describing overall molecular charge distribution as well as anticipating sites of the electrostatic interaction between the TMPyP cation and the respective phosphate anion.

Results and Discussion

Formation of TMPyP Nanoparticles. A series of porphyrin nanoparticles dispersed in water/methanol mixture (9/1) were successfully synthesized. Images a and b in Figure 2show typical STEM images of the organic nanoparticles of TMPyP-**T** sample prepared at ρ = 1 or 1.5, respectively. The particle diameters are in the range of 30−50 nm (average,41 nm; ρ = 1) and 20−40 nm (average; 33 nm: ρ = 1.5) with relatively narrow size distributions. The average diameters are almost similar to each other, in good agreement with those determined by DLS,[16] presenting that of 42 nm (standard deviation; 4.3 nm) or 37 nm (standard deviation; 3.2 nm) for ρ = 1 or 1.5, respectively. Images c and d in Figure 2also show STEM images of the TMPyP-**B** sample prepared at ρ = 1 or 1.5, respectively. The micrographs show that TMPyP-**B** samples have the particle diameters in the range of 20−50 nm (average, 32 nm; ρ = 1) and 30−50 nm (average, 40 nm; ρ = 1.5), suggesting also that the average size is nearly independent of ρ. On the other hand, the average diameters determined by DLS were 280 nm (standard deviation, 17.5 nm) for ρ = 1 and 151 nm (standard deviation, 19.1 nm) for ρ = 1.5, much larger than those estimated by STEM, suggesting the occurrence of slight agglomeration. Interestingly, the size of the TMPyP nanoparticles was in the range of 30−50 nm in diameter and thus almost independent both on the charge ratio expressed as ρ and on the phosphate structure under the present conditions.[17]

The particle formation processes are expected to begin with rapid nucleation and generation of small electrically neutral ion-pair clusters followed by the slow coalescence

(14) TMPyP is a tetravalent cation while TRISPHAT or BINPHAT anion is monovalent. Hence the aqueous solvent-insoluble ion-pair precipitates (solid products) should in principle have a 1:4 stoichiometry of TMPyP:chiral phosphate because of the electrically neutral character. In the nanoparticle synthesis, to avoid the presence of residual free TMPyP monomers (or, to completely convert free TMPyP monomers to nanoparticles) in the water/methanol (9/1) solution, we set the ρ value to 1 or 1.5 (namely, loaded [TMPyP]:[phosphate] = 1:4 or 1:6, respectively).

(15) Frisch, M. J.; Trucks, G. W.; Schlegel, H. B.; Scuseria, G. E.; Robb, M. A.; Cheeseman, J. R.; Montgomery, Jr., J. A.; Vreven, T.; Kudin, K. N.; Burant, J. C.; Millam, J. M.; Iyengar, S. S.; Tomasi, J.; Barone, V.; Mennucci, B.; Cossi, M.; Scalmani, G.; Rega, N.; Petersson, G. A.; Nakatsuji, H.; Hada, M.; Ehara, M.; Toyota, K.; Fukuda, R.; Hasegawa, J.; Ishida, M.; Nakajima, T.; Honda, Y.; Kitao, O.; Nakai, H.; Klene, M.; Li, X.; Knox, J. E.; Hratchian, H. P.; Cross, J. B.; Bakken, V.; Adamo, C.; Jaramillo, J.; Gomperts, R.; Stratmann, R. E.; Yazyev, O.; Austin, A. J.; Cammi, R.; Pomelli, C.; Ochterski, J. W.; Ayala, P. Y.; Morokuma, K.; Voth, G. A.; Salvador, P.; Dannenberg, J. J.; Zakrzewski, V. G.; Dapprich, S.; Daniels, A. D.; Strain, M. C.; Farkas, O.; Malick, D. K.; Rabuck, A. D.; Raghavachari, K.; Foresman, J. B.; Ortiz, J. V.; Cui, Q.; Baboul, A. G.; Clifford, S.; Cioslowski, J.; Stefanov, B. B.; Liu, G.; Liashenko, A.; Piskorz, P.; Komaromi, I.; Martin, R. L.; Fox, D. J.; Keith, T.; Al-Laham, M. A.; Peng, C. Y.; Nanayakkara, A.; Challacombe, M.; Gill, P. M. W.; Johnson, B.; Chen, W.; Wong, M. W.; Gonzalez, C.; Pople, J. A. Gaussian 03; Gaussian, Inc.: Wallingford, CT, 2004.

(16) Water/methanol (9/1 v/v) mixture was used as a solvent for the DLS measurements, so the literature values (see ref 16b) of the viscosity and diffusion coefficient for the mixture, 11.6×10^{-3} cP and 1.32×10^{-9} m^2/s, respectively, were used. (b) Wensink, E. J. W.; Hoffmann, A. C.; van Maaren, P. J.; van der Spoel, D. *J. Chem. Phys.* **2003**, *119*, 7308.

(17) On the basis of our previous studies (see ref 11), mean size of the ion-based organic nanoparticles can be a function of the excess anion concentration (or ρ value) probably due to the anion adsorption onto the nanoparticle surfaces, which may alter the surface charge density or surface electric double-layer screening. In the present cases, however, the lack of size dependence on ρ and the resultant similarity in the spectroscopic nature were observed, suggesting that the surface state or composition of the nanoparticles is also independent of ρ.

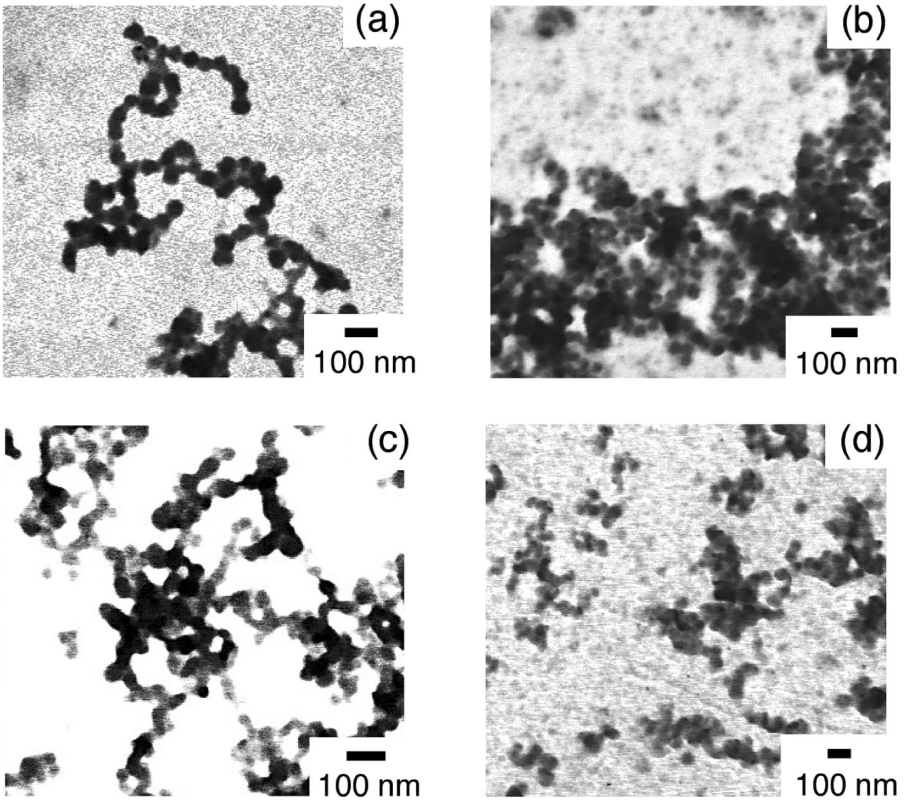

Figure 2. STEM images of the synthesized (a, b) TMPyP-**T** and (c, d) TMPyP-**B** nanoparticle samples.

of these initial clusters into larger particles.[11,18] Once a poor solvent (water) is added into the methanol solution containing TMPyP and phosphate, the TMPyP cation and the hydrophobic phosphate anions first contact with each other to form an ion-pair adduct due to the strong electrostatic attraction. The electrically neutral contact ion pairs aggregate themselves by van der Waals attractive interaction to produce nuclei, followed by the growth of nuclei into aqueous solvent-insoluble larger particles.[11] PVP is found to be capable of stabilizing ion-based organic nanoparticles, as is the case of many metal and semiconductor nanoparticles because of its steric effects.[19] The counteranion dependence on the agglomeration mode of nanoparticles implies the difference in the interparticle attractive force is probably due to the surface state of the particles.

Characterization. To examine the composition of the nanoparticle species, solid-state products formed by the ion-association reaction at $\rho = 1$ were collected using a membrane filter. It was followed by UV−vis spectroscopic measurements since not only TMPyP but also TRISPHAT and BINPHAT have characteristic electronic absorption features. Note that no PVP was added to make the solid-state products grow to be large in size.

We first measured electronic absorption spectra of the native compounds for comparison. Panels a and b in Figures 3show absorption spectra of native TMPyP (PTS salt) and TRISPHAT (BINPHAT) (TBA salt) in methanol, respectively. Figure 3c exhibits the spectrum of pure TBA•PTS dissolved in water. The electronic spectrum of the monomeric TMPyP features several characteristic bands of porphyrin, namely, Q (515, 552, 590, 646 nm), B (424 nm), N (360 nm), and L bands (305 nm), are observed.[20] In Figure 3b, the peak at around 300 or 330 nm (indicated by an arrow) is characteristic to the chromophore in TRISPHAT or BINPHAT, respectively. Note that the naphthalene chromophore consists of ^1L_b, ^1L_a, and ^1B_b ($\pi-\pi^*$) transitions at around 330, 285, and 220 nm, respectively, in the electronic spectrum,[21] so the peak at 330 nm observed for the native BINPHAT is ascribed to the ^1L_b transition of a naphthyl group. We can assign the peak at 300 nm observed for the native TRISPHAT to an $n-\pi^*$ transition based on quantum chemical HOMO and LUMO calculations (see the Supporting Information for detail). Meanwhile in pure TBA·PTS, the absorption peak at 220 nm is due to the phenyl moiety in PTS.

We next obtained absorption spectra of the filtrate (supernatant) solution (Figure 3e) and the collected solid products dissolved in methanol or ethanol completely (Figure 3d). Figure 3d clearly demonstrates that the products are composed solely of TMPyP cations and TRISPHAT (or BINPHAT) anions, which is evidenced by the characteristic peak positions of the constituent

(18) Horn, D.; Rieger, J. *Angew. Chem., Int. Ed.* **2001**, *40*, 4330.
(19) (a) Si, R.; Zhang, Y.; You, L.; Yan, C. *J. Phys. Chem. B* **2006**, *110*, 5994. (b) Vinodgopal, K.; He, Y.; Ashokkumar, M.; Grieser, F. *J. Phys. Chem. B* **2006**, *110*, 3849. (c) Paredes, J. I.; Suarez-Garcia, F.; Villar-Rodil, S.; Martinez-Alonso, A.; Tascon, J. M. D. *J. Phys. Chem. B* **2003**, *107*, 8905. (d) Gabaston, L. I.; Jackson, R. A.; Armes, S. P. *Macromolecules* **1998**, *31*, 2883.
(20) Anex, B. G.; Umans, R. S. *J. Am. Chem. Soc.* **1964**, *86*, 5026.
(21) Jaffe, H. H.; Orchin, M. *Theory and Applications of Ultraviolet Spectroscopy*; Wiley: New York, 1962.

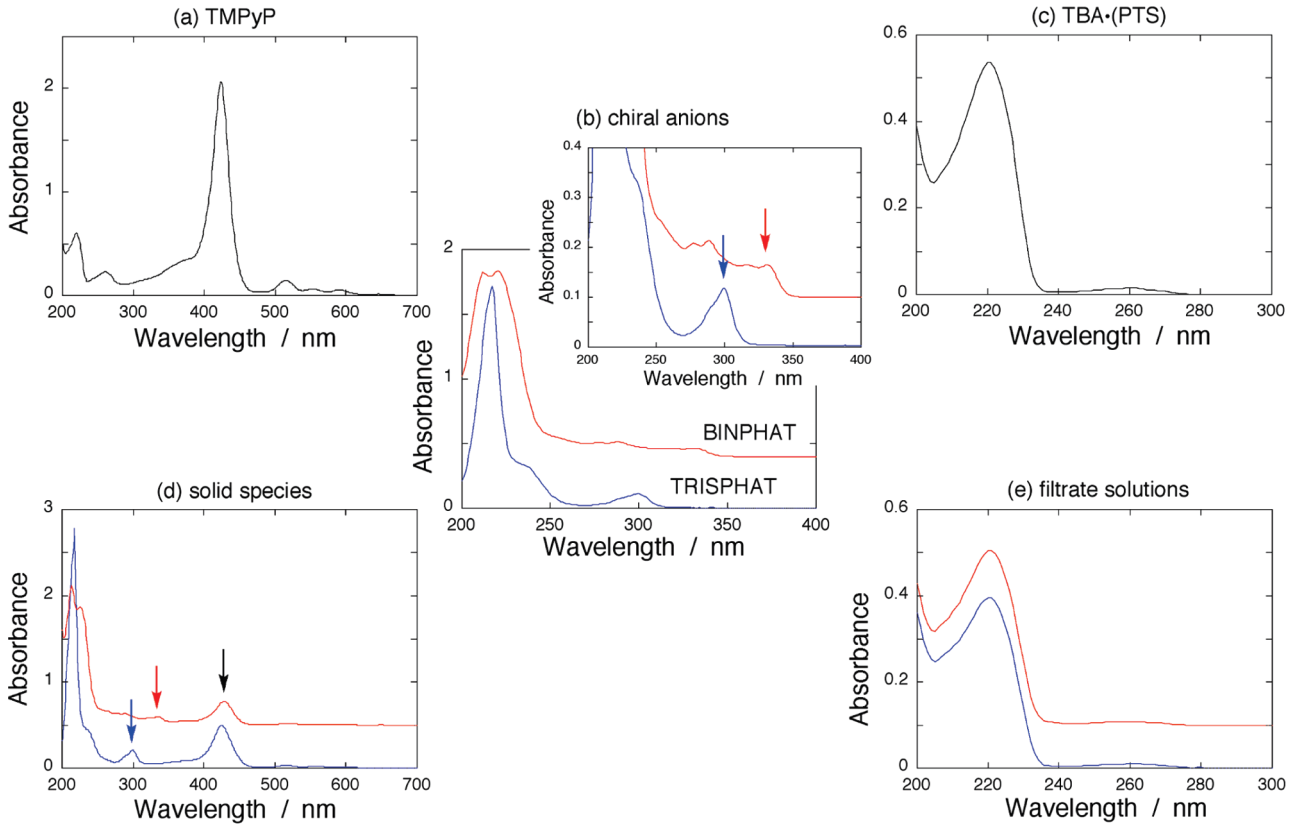

Figure 3. Absorption spectra of (a) native TMPyP in methanol solution, (b) native TRISPHAT and BINPHAT in methanol, (c) TBA•PTS in water, (d) collected solid species dissolved in methanol (TMPyP/TRISPHAT) or ethanol (TMPyP/BINPHAT), and (e) filtrate (supernatant) solution. In c and d, the blue or red curves represent the spectra for the TMPyP/TRISPHAT or TMPyP/BINPHAT system, respectively.

materials (see arrows in the figure).[22] On the other hand, from panels c and e in Figure 3, we know that the filtrate solutions include only TBA and PTS since the absorption spectra completely agreed with that of pure TBA·PTS. Hence we can conclude that the solid-phase porphyrin nanoparticles consist of ion-pair aggregates between TMPyP cations and TRISPHAT (or BINPHAT) anions. It is worth noting here that these solid products were revealed to be amorphous by polarized-light microscopy. See the Supporting Information for more detail.

Optical Properties of TMPyP Nanoparticles. A series of UV−vis absorption spectra of the TMPyP-**T** and TMPyP-**B** nanoparticle samples are shown in panels a and b in Figure 4, respectively. The spectrum of native TMPyP (=monomer species) in water/methanol solution (9/1) is also added in each figure. In all samples, the overall spectral features were similar to each other, but the Soret (or B) and Q bands of the nanoparticle samples exhibited a large bathochromic shift compared to those of the porphyrin monomer in solution: For example, the peak position of the Soret band appeared at 425 nm for the solution-phase TMPyP monomer, whereas that appeared at 446 or 438 nm for the TMPyP-**T** or TMPyP-**B** samples, respectively. The shift in the peak positions proves the electrostatic interaction between the TMPyP cation and the phosphate anion, resulting from the formation of ion-based nanoparticles.[23] Although the Soret peak position was independent of ρ under the same counteranions, as expected from their particle size similarity,[17] it strongly depended on the type of the counteranions used, that is, TMPyP-**T** samples exhibited more red-shifted absorption than TMPyP-**B**, indicating that the interionic interaction in TMPyP/TRISPHAT would be stronger than that in TMPyP/BINPHAT.

It has been proposed that the peak position of the Soret band of porphyrins is a function of various factors including (i) solvent polarity (matrix effect), (ii) protonation of the free-base pyrrole nitrogen, (iii) external electric field, (iv) ruffled/saddled structure of the porphyrin ring, and (v) flattening of the meso-substituents with respect to the

(22) On the basis of Lambert−Beer's law, the absorbance ratio of two characteristic peaks of TMPyP and TRISPHAT (or BINPHAT), A_{425}/A_{300} (or A_{425}/A_{335}), respectively, where a number in subscript denotes the characteristic peak wavelength, should have a certain constant value when the molar ratio of TMPyP to TRISPHAT (or BINPHAT) is 1:4 (or $\rho = 1$). We experimentally determined the A_{425}/A_{300} (or A_{425}/A_{335}) value of ~3.0 (or ~3.6) in methanol solution. In comparison to Figure 3a, almost no peak shift of the Soret bands was observed in Figure 3d, but the values A_{425}/A_{300} and A_{425}/A_{335} estimated from Figure 3d were ~2.5 and ~3.0, respectively, slightly smaller than those expected even though experimental errors are considered. This may be due to the existence of adsorption or inclusion of the phosphate on/in the precipitates.

(23) To confirm whether the porphyrin moieties are self-aggregated or not within the nanoparticles, we carried out fluorescence measurements. The results are shown in the Supporting Information. The spectral shapes of all nanoparticle samples were quite similar but exhibited a considerable red shift compared to that of the TMPyP monomer in water/methanol (9/1) solution (Stokes shift of ~18 nm in the $Q(0,0)$ fluorescence bands), proving the absence of self-aggregates (J-aggregates) because the J-aggregate exhibits almost no Stokes-shifted strong fluorescence.

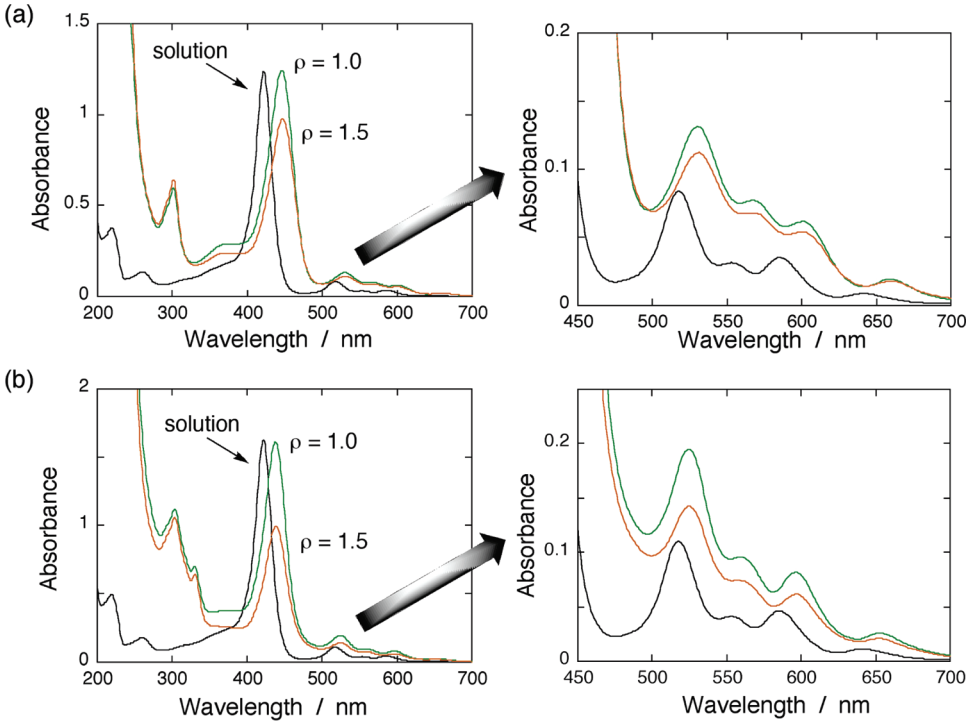

Figure 4. Absorption spectra of (a) TMPyP-**T** and (b) TMPyP-**B** nanoparticle samples. The spectrum of native TMPyP in water/methanol mixture (9/1) is also shown in each figure.

plane of the porphyrin ring.[24] Among them, it is conceivable that factors i−iii are unable to contribute to the present large red shift of the Soret band (~21 nm for TMPyP-**T** and ~13 nm for TMPyP-**B** samples), because (i) it is revealed that the amount of the red shift is very small (≲2 nm) even when the solvent polarity is largely varied;[25] (ii) the acid dissociation constant of TMPyP is reported to be ~1.3 (in water at 25 °C), so the protonation scheme is unlikely under the present experimental conditions;[26] (iii) the strong electric field probably induced by adjacent counteranions tends to blue-shift the Q(0,0) bands, which contradicts our observation.[27] Other factors (iv) and (v) will be discussed in more detail later.

Induced Optical Activity in TMPyP Nanoparticles. Circular dichroism (CD) spectra of native TRISPHAT and BINPHAT (TBA salts) dissolved in methanol are shown in Figure 5a. In TRISPHAT, strong positive and negative bands were obtained for the exciton couplet in the $\pi-\pi^*$ region at shorter and longer wavelengths (207 and 224 nm), respectively,[28] whereas BINPHAT exhibited a bisignate exciton coupling (222 and 233 nm) based on the ^1B_b transition. This bisignate CD signal in the ^1B_b transition with negative Cotton effect at longer wavelength and positive Cotton effect at shorter wavelength indicates the absolute configuration of naphthyl moieties in *R*-configuration where the dihedral angle defined by the two aromatic groups is smaller than about 110°.[29] Figure 5b displays CD spectra of pure methanolic solution containing native TMPyP and TRISPHAT (or BINPHAT) at a molar ratio of 1:4 (or $\rho = 1$). Note that this methanol solution (0.2 mL) was used for mixing with water (1.8 mL) to prepare the relevant organic porphyrin nanoparticles (namely, mother solution). Figure 5b shows that the CD signal is completely silent at the Soret band regions, indicating no interaction between the TMPyP cation and the chiral anion in pure methanol solution.

To obtain insights into the induced optical activity in the porphyrin nanoparticles, CD spectra of the nanoparticle samples were measured. Panels a and b in Figure 6 show the CD spectra of the synthesized TMPyP-**T** and TMPyP-**B** samples in water/methanol (1/9) mixture, respectively. The chiroptical activities induced in the Soret band region were specific, exhibiting split Cotton effects (see the right-side spectra in Figure 6). Note that TMPyP-**T** samples have more complicated CD couplets because of the unsymmetrical CD signals. There has been a few reports on size-defined organic nanoparticles of intrinsically optically active molecules prepared through the reprecipitation method.[30] In contrast, our synthetic strategy for

(24) (a) Takagi, S.; Shimada, T.; Eguchi, M.; Yui, T.; Yoshida, H.; Tryk, D. A.; Inoue, H. *Langmuir* **2002**, *18*, 2265. (b) Ukrainczyk, L.; Chibwe, M.; Pinnavaia, T. L.; Boyd, S. A. *J. Phys. Chem.* **1994**, *98*, 2668. (c) Eguchi, M.; Takagi, S.; Tachibana, H.; Inoue, H. *J. Phys. Chem. Solids* **2004**, *65*, 403. (d) Chernia, Z.; Gill, D. *Langmuir* **1999**, *15*, 1625.(e) In ref 24d, PM3 modeling as applied to the conformational analysis of porphyrin molecules. (f) Kuykendall, V. G.; Thomas, J. K. *Langmuir* **1990**, *6*, 1350. (g) Karki, L.; Vance, F. W.; Hupp, J. T.; LeCours, S. M.; Therien, M. J. *J. Am. Chem. Soc.* **1998**, *120*, 2606. (h) Yao, H.; Kobayashi, S.; Kimura, K. *Chem. Lett.* **2008**, *37*, 594. (i) Xu, Y.; Zhao, L.; Bai, H.; Hong, W.; Li, C.; Shi, G. *J. Am. Chem. Soc.* **2009**, *131*, 13490.
(25) Renge, I. *J. Phys. Chem.* **1993**, *97*, 6582.
(26) Kano, K.; Minamizono, H.; Kitae, T.; Negi, S. *J. Phys. Chem. A* **1997**, *101*, 6118.
(27) Manas, E. S.; Vanderkooi, J. M.; Sharp, K. A. *J. Phys. Chem. B* **1999**, *103*, 6334.
(28) Mason (Banus), J.; Mason, S. F. *Tetrahedron* **1967**, *23*, 1919.
(29) Mason, S. F.; Seal, R. H.; Roberts, D. R. *Tetrahedron* **1974**, *30*, 1671.

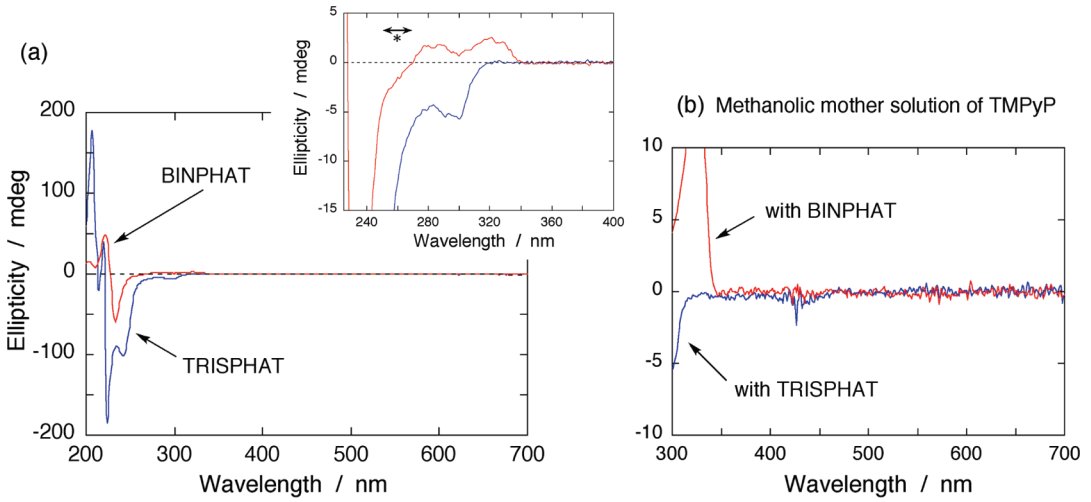

Figure 5. (a) CD spectra of native TRISPHAT and BINPHAT in methanol. The inset shows the magnified spectra in the wavelength region of 230−400 nm. (b) CD spectrum of a mixture of native TMPyP and TRISPHAT (or BINPHAT) at the molar ratio of 1:4 in methanol, corresponding to the mother solution for preparing the nanoparticles at $\rho = 1$.

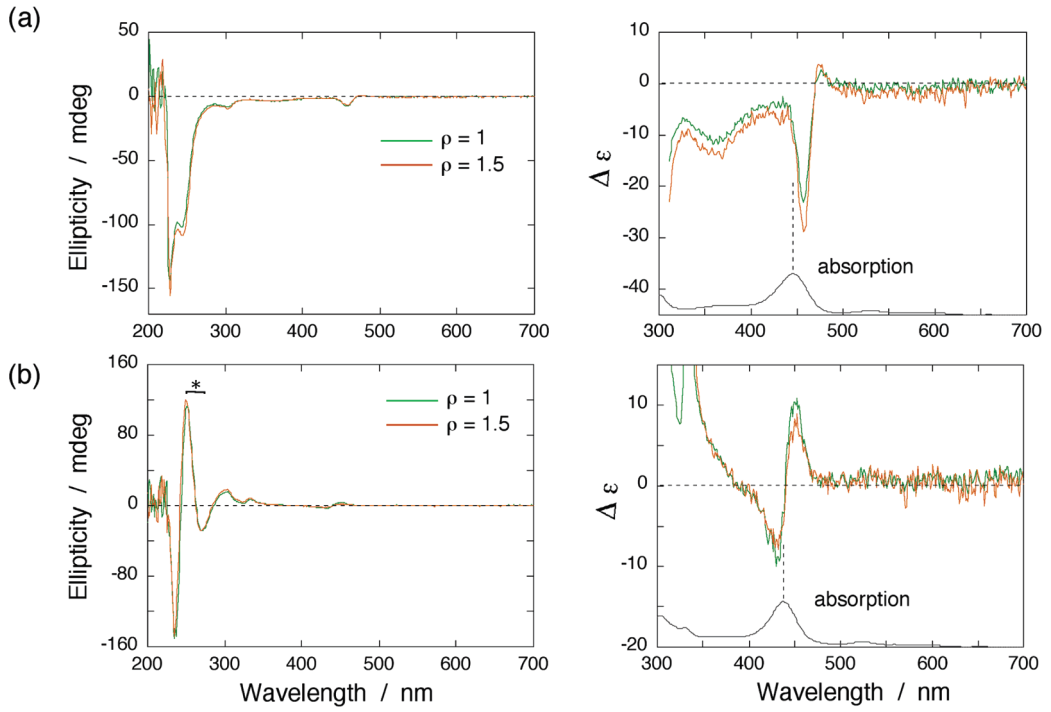

Figure 6. CD spectra of (a) TMPyP-**T** and (b) TMPyP-**B** nanoparticle samples. The right-handed spectra are magnification around the Soret band region along with the corresponding absorption spectra.

organic nanoparticles with induced optical activity has advantages in the fact that chiroptical properties can be tuned by the chiral counterions as well as the chromophoric molecules with desirable transition or energy.

Despite an opposite helicity of TRISPHAT and BINPHAT, the induced CD signals observed at the Soret band region did not satisfy the opposite correlation. This is probably due to the presence of *R*-binaphthyl group in BINPHAT. In other words, the induced chiroptical response in ion-based organic nanoparticles is more sensitive to the surrounding counterion species compared to the optical (absorption) signal, and thus can provide important information on the local environments around the chromophore, as is often the case with natural biosystems.[9]

It is interesting to note that a remarkable amplification of the CD response with split Cotton effects in the ^1L_a transition of naphthyl moiety was observed in the TMPyP-**B** samples when compared to the small CD signal of the native BINPHAT molecule (see the region marked by "*" in Figure 6b and compare with that in the inset in Figure 5a). This chiroptical signal enhancement is unlikely due to both a fixation of the binaphthyl group and a intermolecular interaction between the binaphthyl groups in the solid-state nanoparticle, because the enhancement has

(30) (a) Zhang, Y.; Yang, W.; Tian, Z.; Yao, J. *Talanta* **2005**, *67*, 524. (b) Xi, L.; Fu, H.; Yang, W.; Yao, J. *Chem. Commun.* **2005**, 492.

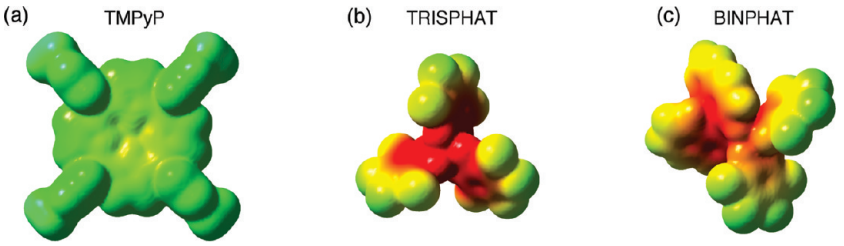

Figure 7. Electrostatic potential surface maps for (a) TMPyP, (b) TRISPHAT, and (c) BINPHAT. Different colors were used to identify different potentials; the most negative potential is colored "red" and the most positive potential is colored "blue".

never been detected in nanoparticles of a binaphthyl derivative.[30a] The origin of this amplification may not be clear at present, but this phenomenon should indicate a strong electric transition dipole coupling that involves the ^1L_a transitions of the naphthyl groups and transitions of porphyrin moieties in nanoparticles.

Conformational Change of Molecular TMPyP in the presence of a Chiral Anion: Quantum Chemical Investigations. To examine whether the molecular structure of cationic TMPyP is changeable by the presence of a counteranion such as TRISPHAT or BINPHAT, and to evaluate the difference in the interactions between TMPyP/TRISPHAT and TMPyP/BINPHAT, we optimized the ground-state geometry of an ion-pair complex of TMPyP−X (X = TRISPHAT or BINPHAT) using the semiempirical PM3 calculations.[24d] Electrostatic potential surfaces (EPS) of the respective ions were also calculated and mapped onto the molecular electron density. Note that we made a structural model of the 1:1 complex to simply examine how one counteranion in the vicinity of tetracationic TMPyP influences the geometry of the porphyrin ring. Figures 7a−c show the EPS maps for TMPyP, TRISPHAT, and BINPHAT, respectively. Different colors are used to identify different potentials; the most negative potential is colored "red" and the most positive potential "blue". Figure 8a displays the optimized structure of the 1:1 complex of TMPyP−TRISPHAT or TMPyP−BINPHAT.

According to Figure 7, the weakly positive electrostatic potential appears to be almost over the macrocycles of TMPyP (that is, diffusive) probably due to the electron-withdrawing nature of pyridinium groups, but the most positive potentials lie around four methylpyridinium substituents. TRISPHAT bears the most negative potential region at around the center of the anion, whereas BINPHAT, with a diffusive potential gradient, has the most negative potential region at around the binaphthyl moiety of a π-donating substituent. Therefore, from the standpoint of the electrostatic potential, stronger binding or interaction is anticipated for the TMPyP/TRISPHAT system than that for TMPyP/BINPHAT. On the basis of Figure 8a, indeed, the BINPHAT molecule sits in between two methylpyridinium groups of TMPyP and the binaphthyl group points toward one of the pyridinium moieties, whereas the TRISPHAT molecule is much more closely approached (protruded) by the porphyrin macrocycle.

In the structure of free (liberated) TMPyP cation (Figure 7a), four methylpyridinium groups are stable to be almost perpendicular to the plane of the porphine ring.[24d]

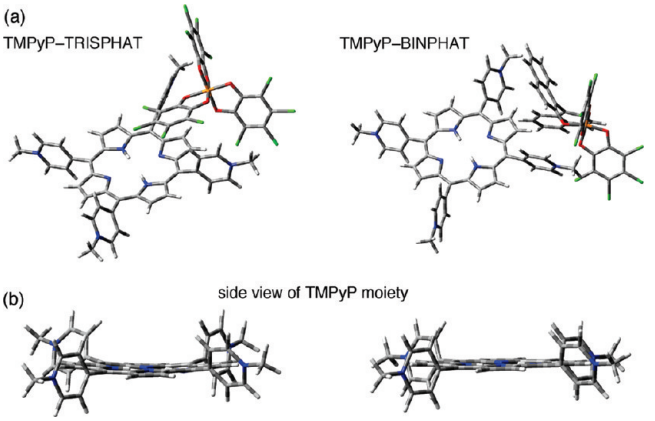

Figure 8. (a) Optimized structure of the 1:1 complex of TMPyP−TRISPHAT or TMPyP−BINPHAT calculated at the PM3 level. (b) Side view of the TMPyP structure separated from the optimized ion-pair complexes shown in a.

However, on the basis of the optimized structures of both the 1:1 ion-pair complexes, a flattening of TMPyP is obvious, that is, the dihedral angles (θ_d) of the meso-substituted pyridinium planes versus the plane of the porphyrin ring became smaller than that of free TMPyP. It is generally accepted that the pyridinium flattening induces an increase in the area of delocalization of the π-electrons in porphyrin, over the entire molecular plane, leading to the red shift of the Soret band.[25] Previous calculations also suggest that θ_d of ~60° causes a ~30 nm red shift in the Soret band of TMPyP.[24d] Therefore, one major reason for the large red shift of the Soret band should be the flattening of the TMPyP molecule in the nanoparticle.

In the 1:1 complex of TMPyP−X (X = TRISPHAT or BINPHAT), the degree of flattening, which can be estimated by averaging four θ_d obtained, was about 75−79° and thus similar to each other at the PM3 level. Hence to better understand the details of the observed red shift of the Soret bands, we further examined the TMPyP structures in these complexes from a viewpoint of macrocycle deformation. Figure 8b displays the side views of TMPyP alone extracted from these complexes. Interestingly, it is evident that the porphyrin macrocycle in TMPyP−TRISPHAT has large saddling distortion as compared to that in TMPyP−BINPHAT. This is probably caused by stronger interaction between TMPyP and TRISPHAT, as is expected from the electrostatic potential surfaces. It has also been revealed that nonplanar distortions (ruffling and saddling) of the porphyrin skeleton bring about red shifts in the electronic absorption spectra due to destabilization

of the porphyrin HOMOs.[31] Therefore, it is reasonable to consider that both flattening of *meso*-substituents and saddling/ruffling deformation of porphyrin macrocycle are responsible for the larger bathochromic shift observed in TMPyP-**T** samples as compared to the case of TMPyP-**B** samples.

Possible Origin of the Induced Circular Dichroism in the Soret Band. We demonstrated that optical activity could be successfully induced in porphyrin nanoparticles prepared by the chiral ion-association method. Although it may be difficult at present to fully determine the underlying mechanisms, two possible origins, in principle, can be considered to account for the induction of optical activity in the porphyrin chromophore; conformational effect of porphyrin, or chiral transfer from counteranions. The former includes (i) asymmetric puckering (distortion) of the porphyrin plane caused by ion-pair interaction, and (ii) exciton coupling where transition dipoles of the two (or more) chirally arranged porphyrins interact with each other in the nanoparticle.[32] The latter includes (iii) the coupling between the magnetic transition and/or electric transition dipole moments of the counteranions (matrices) and the electric transition moment of the porphyrin π-system. Mechanism iii is based on the theoretical considerations that the rotational strength can be calculated from the imaginary part of the scalar product of the electric and magnetic dipole transition moments.[33]

In the CD spectra of the synthesized TMPyP nanoparticles, magnitudes of the chiroptical response or differential molar dichroic absorption coefficients ($\Delta\varepsilon$) in the Soret band region are not so large ($\Delta\varepsilon \approx \pm 10-30$ M^{-1} cm^{-1}). Because the exciton coupling between chirally stacked porphyrins yields very large magnitudes of the chiroptical responses ($\Delta\varepsilon \approx 1 \times 10^3$, about 100 times larger than that obtained for our nanoparticle systems), the above-mentioned mechanism (ii), that is, porphyrin stacking possibility in a chiral fashion, should be ruled out. This means that TMPyP molecules are not strongly interacted with each other in the nanoparticles.

The situation of TMPyP in chiral ion-based organic nanoparticles is somewhat similar to that of heme in myoglobin.[9] Regarding the mechanism i, a theoretical study on the effect of heme ruffling on its rotational strength would be helpful:[34] It is reported that deviations from porphyrin planarity introduce chirality in the heme and make the two Soret transitions (two nearly degenerate components (termed as B_x and B_y) that are polarized in the plane of the porphyrin ring and perpendicular to each other) distinct, resulting in a net intrinsic rotational strength, leading to observable Soret CD signals.[34] Importantly, the two orthogonally polarized transitions have intrinsic rotational strengths that are opposite in sign (split type), so the net rotational strength becomes small in magnitude due to the their cancellation but has maximal magnitudes of $\sim 4.5 \times 10^{-39}$ in cgs units (absolute value).[34] Note that the net rotational strength shows no correlation with the average twist (deformation) angle of the macrocycle.[34] The rotational strength is estimated by integrating the intensity under a single band of CD signal, so that we can roughly calculate the maximal absolute values of the rotational strength of the Soret band as $\sim 1.2 \times 10^{-39}$ and $\sim 0.7 \times 10^{-39}$ cgs for the TMPyP−X (X = TRISPHAT and BINPHAT) samples, respectively. These values are smaller than those obtained theoretically but in the same order.[34] Hence the mechanism (i) would contribute to the observed chiroptical response in the TMPyP nanoparticles if the saddling/ruffling deformation of porphyrin ring is possible.

In many aromatic ketones, the coupling between the magnetic transition moment of a carbonyl group and the electric transition moment of a phenyl group is an origin of the optical activity.[35] Similarly, in amino acid−porphyrin supramolecular systems, it is found that the coupling between the magnetic transition moment of the carbonyl $n-\pi^*$ transition and the electric transition moment of the porphyrin Soret band can be attributed to the induced CD signals with split Cotton effects when the two chromophores are fixed.[36] In addition to the influence of the $n-\pi^*$ magnetic transition, aromatic chromophores in the amino acid make an additional contribution to their chiroptical signals, resulting in the $\Delta\varepsilon$ value of about $\pm 10-30$ $M^{-1}cm^{-1}$.[36] On this basis, it is also possible that the induced optical activity in the Soret band is caused by the mechanism (iii), namely, the coupling between the magnetic transition moment ($n-\pi^*$) and/or electric transition moment ($\pi-\pi^*$) of the aromatic phosphate, and the electric transition moment of the porphyrin Soret band.[37] This is corroborated by the presence of strong interionic interactions between the TMPyP cations and the chiral anions in the nanoparticles. Further investigation would be necessary to determine the contributions from each of these possibilities in ion-based organic nanoparticles. In summary, the present tactic using ion-association of achiral chromophore with chiral counterions has proven to be a powerful tool to yield optically active organic nanoparticles in a simple and biomimetic manner. Optical and chiroptical properties can be tuned by controlling a combination of the chromophore and chiral counterion. Moreover, as a material design strategy, chiral amplification will be expected when a chiral polymer is additionally used to stabilize the organic nanoparticle systems, which may arise from the cooperative effect of asymmetric environments possessing both chiral counterions and polymers.

(31) (a) Parusel, A. B. J.; Wondimagegn, T.; Ghosh, A. *J. Am. Chem. Soc.* **2000**, *122*, 6371. (b) DiMagno, S. G.; Wertsching, A. K.; Ross, C. R., II *J. Am. Chem. Soc.* **1995**, *117*, 8279.
(32) Sebek, J.; Bour, P. *J. Phys. Chem. A* **2008**, *112*, 2920.
(33) Rosenfeld, L. *Z. Phys.* **1928**, *52*, 161.
(34) Kiefl, C.; Sreerama, N.; Haddad, R.; Sun, L.; Jentzen, W.; Lu, Y.; Qiu, Y.; Shelnutt, J. A.; Woody, R. W. *J. Am. Chem. Soc.* **2002**, *124*, 3385.
(35) Moscowitz, A.; Mislow, K.; Glass, M. A.; Djerassi, C. *J. Am. Chem. Soc.* **1962**, *84*, 1945.
(36) (a) Mizutani, T.; Ema, T.; Yoshida, T.; Renné, T.; Ogoshi, H. *Inorg. Chem.* **1994**, *33*, 3558. (b) Huang, X.; Nakanishi, K.; Berova, N. *Chirality* **2000**, *12*, 237.
(37) The lowest HOMI−LUMO excitation in TRISPHAT would be the $n-\pi^*$ transition. See the Supporting Information for detail. The HOMO−LUMO transition in BINPHAT is $\pi-\pi^*$ transition of naphthalene moiety.

Conclusion

Ion association between tetracationic *meso*-tetrakis-(1-methylpyridinium-4-yl) porphine (TMPyP) and a chiral anion of TRISPHAT with Δ-configuration or BINPHAT with Λ-configuration, in the presence of poly-(vinylpyrrolidone) (PVP), produced organic nanoparticles of TMPyP (30−50 nm in diameter) with induced optical activity in water/methanol mixture. The peak positions of the Soret band in the nanoparticles exhibited a large bathochromic shift in comparison with that of the porphyrin monomer in solution. Simple quantum chemical calculations showed that the *meso*-substituent flattening as well as ruffling/saddling deformation of the porphyrin macrocycle had a strong influence on the red shift of absorption. The induced circular dichroism (CD) signals of the TMPyP nanoparticles exhibited split Cotton effects at the Soret band regions with their $|\Delta\varepsilon|$ values of about 10−30 $M^{-1}cm^{-1}$. The CD split mode was different between the nanoparticles of TMPyP/TRISPHAT and TMPyP/BINPHAT systems, suggesting different interionic interactions. We proposed that the induced chiroptical response observed in the nanoparticles was a combination of (i) the coupling between the magnetic transition moment and/or electric transition moment of the aromatic phosphate, and the electric transition moment of the porphyrin Soret band, and (ii) a chiral distortion of the TMPyP chromophore caused by the peripheral matrix. We expect that the chiral ion association technique will play a vital role for the biomimetic syntheses of various organic nanoparticles in the future.

Acknowledgment. The present work was financially supported by Grant-in-Aids for Scientific Research (C: 22510104 (H.Y.)) from Japan Society for the Promotion of Science (JSPS).

Supporting Information Available: Polarized-light microscopy observations of the solid-state products of TMPyP/TRISPHAT and TMPyP/BINPHAT, HOMO and LUMO of the TRISPHAT molecule obtained on the basis of B3LYP/6-31+G* calculations, and steady-state fluorescence spectra of TMPyP-**T** and TMPyP-**B** nanoparticle samples (PDF). This material is available free of charge via the Internet at http://pubs.acs.org.